

A Possible Substellar Companion to the Intermediate-mass Giant HD 175679

Liang Wang^{1,2}, Bun’ei Sato³, Gang Zhao¹, Yujuan Liu¹, Kunio Noguchi⁴, Hiroyasu Ando⁴, Hideyuki Izumiura⁵, Eiji Kambe⁵, Masashi Omiya³, Hiroki Harakawa³, Fan Liu^{1,2}, Xiaoshu Wu^{1,2}, Yoichi Takeda⁴, Michitoshi Yoshida⁶ and Eiichiro Kokubo⁴

¹ Key Laboratory of Optical Astronomy, National Astronomical Observatories, Chinese Academy of Sciences, A20, Datun Road, Chaoyang District, Beijing 100012, China; wangliang@nao.cas.cn

² Graduate University of the Chinese Academy of Sciences, 19A Yuquan Road, Shijingshan District, Beijing 100049, China

³ Department of Earth and Planetary Sciences, Graduate School of Science and Engineering, Tokyo Institute of Technology, 2-12-1 Ookayama, Meguro-ku, Tokyo 152-8551, Japan

⁴ National Astronomical Observatory of Japan, National Institutes of Natural Sciences, Mitaka, Tokyo 181-8588, Japan

⁵ Okayama Astrophysical Observatory, National Astronomical Observatory of Japan, National Institutes of Natural Sciences, Asakuchi, Okayama 719-0232, Japan

⁶ Hiroshima Astrophysical Science Center, Hiroshima University, 1-3-1 Kagamiyama, Higashi-Hiroshima 739-8526, Japan

Abstract We report the discovery of a substellar companion around the intermediate-mass giant HD 175679. Precise radial velocity data of the star from Xinglong Station and Okayama Astrophysical Observatory (OAO) revealed a Keplerian velocity variation with an orbital period of 1366.8 ± 5.7 days, a semiamplitude of $380.2 \pm 3.2 \text{ m s}^{-1}$, and an eccentricity of 0.378 ± 0.008 . Adopting a stellar mass of $2.7 \pm 0.3 M_{\odot}$, we obtain the minimum mass of the HD 175679 b is $37.3 \pm 2.8 M_{\text{J}}$, and the semimajor axis is $3.36 \pm 0.12 \text{ AU}$. This discovery is the second brown dwarf companion candidate from a joint planet-search program between China and Japan.

Key words: stars: individual: HD 175679 — stars: brown dwarfs — techniques: radial velocities

1 INTRODUCTION

Brown dwarfs are widely known as “failed stars”, with masses falling between the deuterium-burning limit ($\sim 13 M_{\text{J}}$) and the hydrogen-burning limit ($\sim 80 M_{\text{J}}$). A brown dwarf with a mass of $15 M_{\text{J}}$ and a separation of $\sim 3 \text{ AU}$ in a circular orbit around a solar-mass star causes a radial-velocity semi-amplitude of stellar motion of above 200 m s^{-1} , if seen along the orbital plane, which is easy to be detected with precise radial velocity techniques. However, compared with the number of planetary and stellar companions, the brown dwarf-mass companions revealed by Doppler surveys are rare. Grether & Lineweaver (2006) estimated that less than 1% of Sun-like stars harbor brown dwarf companions. This rate is significantly lower than that of harboring stellar ($11 \pm 3\%$) or giant planetary ($5 \pm 2\%$) companions (Grether & Lineweaver, 2006). Marcy & Butler (2000) also reported only 0.5% of main sequence stars have brown dwarf-mass companions within 3 AU. Such a deficit between the planetary and stellar mass in the mass distribution of companions is called the “brown dwarf desert”. The paucity of brown dwarf

companions may imply two distinct formation mechanisms: core-accretion model (e.g. Ida & Lin 2004, Alibert et al. 2005), which is thought to be the main mechanism of giant planet formation (e.g. Fischer & Valenti 2005, and references therein), and disk instability model (e.g. Boss 1997), which may dominate the formation processes of brown dwarf or substellar companions.

In the past decades, 7 brown dwarf-mass companions and more than 20 planetary companions around intermediate-mass stars have been detected by several Doppler survey programs (e.g. Frink et al. 2002; Sato et al. 2003, 2008a, 2008b; Setiawan et al. 2003; Hatzes et al. 2005; Lovis & Mayor 2007; Niedzielski et al. 2007; Johnson et al. 2007; Liu et al. 2008, 2009; Omiya et al. 2009; Han et al. 2010). Although the number is still small compared with those around solar-mass stars, some remarkable properties have already been revealed, providing important clues on the physical properties of the proto-planetary disks. For instance, the planet occurrence rate around intermediate-mass stars ($1.3 \sim 1.9 M_{\odot}$) is 10-15% (Döllinger et al. 2009), which is significantly higher than that around solar-mass stars (e.g. Cumming et al. 2008). This can be interpreted by the higher surface densities of protoplanetary disks around more massive stars (Ida & Lin, 2005). Nearly all the substellar companions discovered around intermediate-mass giants have semimajor axes larger than 0.6 AU. The lack of inner planets can be explained by the engulfment by the central stars due to the tidal torque during the RGB phase (Sato et al. 2008a), or formed primordially (Burkert & Ida, 2007). The planet-metallicity correlation for planets around solar-type stars does not seem to exist for those around intermediate-giants (Pasquini et al. 2007; Takeda et al. 2008), and therefore constrain the planet formation model (e.g. Ida & Lin 2004, Boss 1997).

In this paper, we report the detection of a brown dwarf-mass companion candidate to the intermediate-mass giant HD 175679. This is the second brown dwarf candidate and the third discovery of the China-Japan planet search program carried out at Xinglong Station (National Astronomical Observatories, China) and Okayama Astrophysical Observatory (OAO, Japan).

2 OBSERVATIONS

2.1 OAO observations

The Okayama Planet Search Program started in 2001. The program has been carrying out a precise Doppler planet survey of 300 G and K giants using the 1.88m telescope with the High Dispersion Echelle Spectrograph (HIDES: Izumiura 1999) at OAO. In 2007 December, HIDES was upgraded from a single CCD ($2 K \times 4 K$) to a mosaic of three CCDs, which can simultaneously cover a wavelength range of 3750-7500 Å using the RED cross-disperser. We set the slit width to $200 \mu m$ ($0.76''$), giving a spectral resolution ($\lambda/\Delta\lambda$) of 67,000 with 3.3 pixels sampling, and we use an iodine absorption cell (I_2 cell: Kambe et al. 2002) for precise wavelength calibration. The reduction of the echelle spectra is performed using the IRAF¹ software package in the standard manner. The I_2 -superposed (“star+ I_2 ”) spectra are modeled based on the algorithm given by Sato et al. (2002). The stellar template used for radial velocity analysis is extracted by deconvolving an instrumental profile, which is determined by a B-star+ I_2 spectrum, from a pure stellar spectrum taken without I_2 cell. The Doppler precision is less than $6 m s^{-1}$ over a time span of 9 yr. We used the stellar spectra without I_2 cell for abundance analysis (e.g. Takeda et al. 2008, Liu et al. 2010).

2.2 Xinglong Observations

To extend the Okayama Planet Search Program, the Xinglong Planet Search Program started in 2005 under a framework of international collaboration between China and Japan. About 100 G-type giants with magnitudes of $6.0 < V < 6.2$ are being monitored with the 2.16 m telescope and the Coudé Echelle Spectrograph (CES: Zhao & Li 2001) at Xinglong. A part of the sample is also being monitored at OAO in order to confirm the stars’ radial-velocity variability independently and HD 175679 presented

¹ IRAF is distributed by the National Optical Astronomy Observatory, which is operated by the Association of Universities for Research in Astronomy, Inc., under cooperative agreement with the National Science Foundation.

Table 1 Stellar Parameters of HD 175679

Parameter	Value
Spectral Type	G8III
π (mas)	6.23 ± 0.80
V	6.14
$B - V$	0.961
M_V	0.52
BC	-0.318
T_{eff} (K)	4844 ± 100
$\log g$	2.59 ± 0.10
[Fe/H]	-0.14 ± 0.10
v_t (km s $^{-1}$)	1.4 ± 0.2
L (L_{\odot})	66 ± 17
R (R_{\odot})	11.6 ± 1.6
M (M_{\odot})	2.7 ± 0.3
Age (Gyr)	$0.5^{+0.4}_{-0.2}$

in this paper is included in the sample observed both at Xinglong and OAO. The iodine absorption cell attached to CES is a copy of that for HIDES at OAO. We use the blue arm of CES for precise radial velocity measurements, which covers a wavelength range of 3900-7260 Å with a spectral resolution of 40,000 by 2 pixel sampling. Due to the small format of the CCD (1 K × 1 K, with a pixel size of $24 \times 24 \mu\text{m}^2$), only about 470 Å is available for precise radial velocity measurements. The modeling of the star+I₂ spectra and template extraction is based on the method by Sato et al. (2002), giving a radial velocity precision of 20 – 25 m s $^{-1}$ over a time span of 3 yr, which is limited by the low resolution of the spectrograph and the narrow wavelength coverage of the CCD. In March 2009, the CCD was replaced by Princeton Instrument’s VersAarray:2048B equipped with an e2v CCD42-40 image sensor having a pixel size of $13 \times 13 \mu\text{m}^2$, which was provided by the National Astronomical Observatory of Japan (NAOJ). The sampling rate is increased to about 3.9 pixels, although the wavelength coverage nearly does not change. Radial velocity analysis for the data with the new CCD is basically the same as that for the data with the old CCD, but we used the stellar template obtained with the OAO data for the analysis of the Xinglong new data. We achieved a Doppler precision of about 15 m s $^{-1}$ with a typical S/N of 150-200 over a time span of 1 yr.

3 STELLAR PROPERTIES

HD 175679 (HR 7144, HIP 92968, BD +02 3730) is a G8III star with $V = 6.14$, $B - V = 0.96$, and a *Hipparcos* parallax of $\pi = 6.23 \pm 0.8$ mas (ESA 1997), giving the distance of 161 ± 21 pc from the Sun, and the absolute magnitude $M_V = 0.52$. The physical parameters (T_{eff} , [Fe/H], $\log g$, v_t , and M_*) are taken from Liu et al. (2010), who used the stellar spectra obtained without I₂ cell at OAO. The effective temperature ($T_{\text{eff}} = 4844 \pm 100$ K) was derived from color index $B - V$ and the empirical calibration relations of Alonso et al. (1999), and the metallicity [Fe/H]=-0.14 was derived from the equivalent widths measured from the I₂-free spectrum. Surface gravity, $\log g = 2.59 \pm 0.10$, was determined via *Hipparcos* parallax (ESA 1997). The stellar mass $M_* = 2.7 \pm 0.3 M_{\odot}$ was estimated from the Yonsei-Yale stellar evolutionary tracks (Yi et al. 2003). Microturbulent velocity $v_t = 1.4 \pm 0.2$ km s $^{-1}$ was obtained by forcing Fe I lines with different strengths to give the same abundances. The stellar parameters are summarized in Table 1.

4 RADIAL VELOCITIES AND ORBITAL SOLUTION

The observation of HD 175679 was started at OAO and Xinglong Station in 2005. Over a time span of 5 years, we collected a total of 22 radial velocity data points at OAO with a typical S/N of 250 and 31 data points at Xinglong (23 with old CCD and 8 with new CCD) with a typical S/N of 150-200. The radial velocity points are shown in Figure 1 and listed in Table 2 together with their estimated uncertainties.

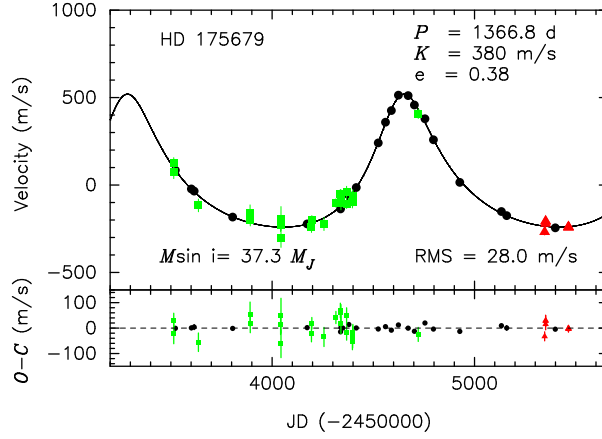


Fig. 1 Radial velocities of HD 175679 observed at OAO (black circles) and Xinglong with old CCD (green squares) and new CCD (red triangles). The Keplerian orbit (solid line) was determined using both the OAO and Xinglong data.

The best-fit Keplerian orbit was derived from both the OAO and Xinglong data using a least-squares method, and is shown in Figure 1 overplotted on the velocity data points. We applied the velocity offset of -177 m s^{-1} and -318 m s^{-1} to Xinglong old and new data respectively, relative to the OAO data in order to minimize reduce χ -squared ($\sqrt{\chi^2_\nu}$) when fitting a Keplerian model to the combined Xinglong and OAO data. The orbital parameters are listed in Table 3, and their uncertainties were estimated using a bootstrap Monte-Carlo approach, subtracting the theoretical fit, scrambling the residuals, adding the theoretical fit back to the residuals and then refitting.

The radial velocity variability can be well fitted as a Keplerian orbit with period $P = 1366.8 \pm 5.7$ days, a velocity semi-amplitude $K_1 = 380.2 \pm 3.2 \text{ m s}^{-1}$, and an eccentricity $e = 0.378 \pm 0.008$. Adopting a stellar mass of $2.7 \pm 0.3 M_\odot$ (Liu et al. 2010), we obtain for the companion a minimum mass $m_2 \sin i = 37.3 \pm 2.8 M_J$ and a semimajor axis $a = 3.36 \pm 0.12 \text{ AU}$. Overall RMS scatter of the residuals was 28.0 m s^{-1} , which was due to the low precision of the Xinglong old data. If we only use the OAO data, the RMS scatter is decreased to 8.4 m s^{-1} , which is consistent with the radial velocity jitter ($\sim 6 \text{ m/s}$) due to stellar oscillations estimated using the scaling relations of Kjeldsen & Bedding (1995).

Table 2: Radial Velocities of HD 175679

JD (−2,450,000)	Radial velocity (m s^{-1})	Error (m s^{-1})	Observatory
3514.29867	76.7	40.2	Xinglong (old)
3514.31969	126.6	29.8	Xinglong (old)
3522.16608	84.5	6.4	OAO
3601.15072	−22.3	6.9	OAO
3615.14723	−34.8	10.0	OAO
3636.04337	−116.4	36.4	Xinglong (old)
3805.33702	−183.1	6.1	OAO
3891.30602	−160.4	47.0	Xinglong (old)
3892.31025	−198.8	35.4	Xinglong (old)
4042.02550	−225.7	40.4	Xinglong (old)
4043.94178	−191.9	68.6	Xinglong (old)
4043.96374	−302.3	54.4	Xinglong (old)

Table 2: continued.

JD (−2,450,000)	Radial velocity (m s^{-1})	Error (m s^{-1})	Observatory
4173.34589	−222.3	5.0	OA0
4194.34042	−237.4	33.8	Xinglong (old)
4196.36671	−197.3	22.7	Xinglong (old)
4256.27293	−222.8	37.8	Xinglong (old)
4315.14228	−102.6	24.0	Xinglong (old)
4337.08455	−53.8	28.7	Xinglong (old)
4338.03334	−136.7	4.8	OA0
4339.99129	−117.3	4.5	OA0
4340.06605	−59.6	32.7	Xinglong (old)
4340.07325	−103.4	38.5	Xinglong (old)
4348.98057	−109.7	4.5	OA0
4368.01697	−39.1	31.8	Xinglong (old)
4368.03145	−105.5	29.0	Xinglong (old)
4379.03102	−58.2	5.5	OA0
4396.96580	−95.7	35.4	Xinglong (old)
4397.94288	−99.2	22.8	Xinglong (old)
4397.95442	−62.7	27.2	Xinglong (old)
4398.97764	−76.1	28.2	Xinglong (old)
4398.99416	−62.7	34.6	Xinglong (old)
4415.89851	−14.3	5.0	OA0
4524.34441	241.0	5.7	OA0
4560.32605	359.0	4.8	OA0
4589.27815	426.0	4.7	OA0
4624.11627	514.0	5.7	OA0
4672.08312	511.3	5.1	OA0
4703.09453	457.6	4.4	OA0
4722.06738	408.2	27.8	Xinglong (old)
4754.97696	379.1	4.8	OA0
4796.88244	258.7	4.9	OA0
4927.32075	15.1	5.0	OA0
5132.92161	−151.7	4.6	OA0
5158.93295	−174.9	9.2	OA0
5346.30620	−267.9	17.9	Xinglong (new)
5351.26229	−208.5	21.9	Xinglong (new)
5351.28343	−220.8	22.3	Xinglong (new)
5351.30453	−205.6	20.3	Xinglong (new)
5399.05791	−244.7	4.5	OA0
5464.00346	−242.4	11.5	Xinglong (new)
5464.02484	−239.0	10.7	Xinglong (new)
5464.04632	−241.5	12.0	Xinglong (new)
5464.06775	−239.4	10.4	Xinglong (new)

5 LINE SHAPE ANALYSES

We performed a spectral line-shape analysis to investigate other causes that could produce apparent radial-velocity variations, such as rotational modulation and pulsation. The high-resolution I_2 -free stellar templates at the peak and valley phases of the observed radial velocities are extracted from several

Table 3 Orbital Parameters of HD 175679 Determined from both Xinglong and OAO Data

Parameter	Value
P (days)	1366.8 ± 5.7
K_1 (m s^{-1})	380.2 ± 3.2
e	0.378 ± 0.008
ω (deg)	346.4 ± 1.3
T_p (JD - 2,450,000)	3263.9 ± 7.6
$a_1 \sin i$ (10^{-3} AU)	44.23 ± 0.43
$f_1(m)$ ($10^{-7} M_\odot$)	61.8 ± 1.7
$M_p \sin i$ (M_J)	37.3 ± 2.8
a (AU)	3.36 ± 0.12
N_{obs}	53
RMS (m s^{-1})	28.0
Reduced $\sqrt{\chi^2_\nu}$	1.5

star + I₂ spectra obtained at OAO. Cross-correlation profiles of the templates were calculated for about 80 spectral segments (4-5 Å width each) in which severely blended lines or broad lines were excluded. We calculated three bisector quantities for the cross-correlation profile of each segment: the velocity span (BVS), which is the velocity difference between two flux levels of the bisector, the velocity curvature (BVC), which is the difference in the velocity span of the upper half and lower half of the bisector, and the velocity displacement (BVD), which is the average of the bisector at three different flux levels. We used flux levels of 25%, 50%, and 75% of the cross-correlation profile to calculate the above three quantities, and the results are plotted in Figure 2. Both BVS and BVC for HD 175679 are identical to zero ($+0.3 \text{ m s}^{-1}$ and -0.1 m s^{-1} on average, respectively), which means the cross-correlation profiles are symmetric. The average BVD of -603.9 m s^{-1} is consistent with the velocity difference between the two templates at the peak and valley phases of the observed radial velocities. As a result, we concluded that the observed radial velocity variations are due to parallel shifts of the spectral lines caused by orbital motion.

6 SUMMARY AND DISCUSSION

We report the discovery of a brown dwarf-mass companion candidate to the intermediate-mass giant HD 175679. This is the second brown dwarf discovered by the joint China-Japan planet search program. It also need to be emphasized that the unknown orbital inclination i leaves the true mass of HD 175679 b uncertain. If the orbit is randomly oriented, there is a 10% chance that the true mass exceeds $80 M_J$ ($i < 28^\circ$), which is the border between brown dwarf and stellar mass regimes.

In Table 4, we listed parameters of discovered brown dwarf-mass companions around intermediate-mass giants and properties of their host stars. The semi-major axes versus eccentricities of brown dwarf companions above are plotted in Figure 3, together with those of planetary companions around intermediate-mass stars ($1.5 M_\odot \leq M \leq 5 M_\odot$). The parameters of companions and host stars are taken from Table 4 and *The Extrasolar Planets Encyclopedia*². As seen in the figure, brown dwarf-mass companions reside in orbits with $a \geq 1.3$ AU, while planetary ones exist in more inner orbits with $a \geq 0.6$ AU. This may reflect the different history of formation and evolution between brown dwarfs and planets.

HD 175679 b has a minimum mass of $37.3 M_J$ orbiting an evolved star with $2.7 M_\odot$, with a period of 1367 days. As the 8th brown dwarf-mass companion candidate to intermediate-mass giants (Hatzes et al. 2005; Lovis & Mayor 2007; Liu et al. 2008; Omiya et al. 2009; Niedzielski et al. 2009; Sato et al. 2010), HD 175679 b is somewhat unique in some respects. Although it has been well known that more massive stars tend to host more massive planets or brown dwarfs than lower-mass stars (Lovis & Mayor

² <http://exoplanet.eu/>, retrieved on 09/May/2010.

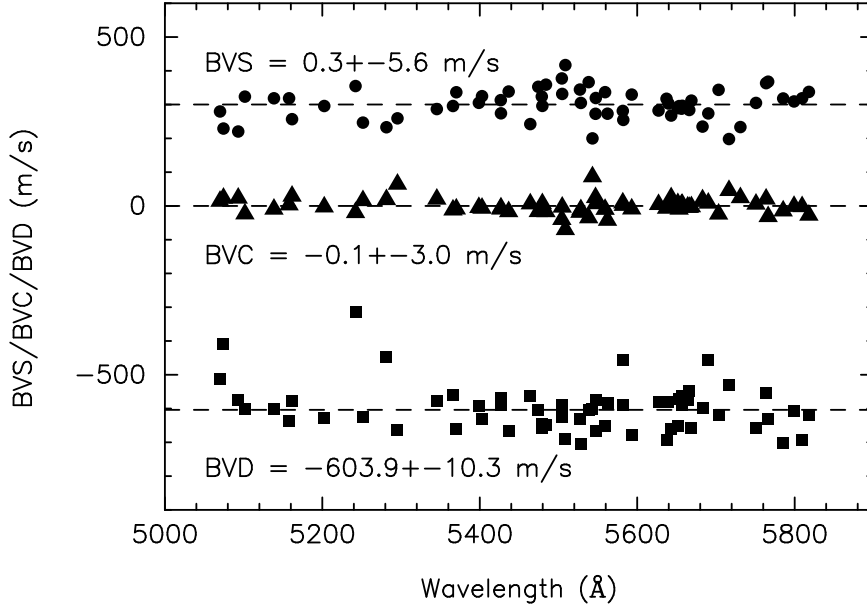


Fig. 2 Bisector quantities of the cross-correlation profiles between the templates of HD 175679 at peak and valley phases of the observed radial velocities. The bisector velocity span (BVS, circles), bisector velocity curvature (BVC, triangles), and bisector velocity displacement (BVD, squares) with average values (dashed lines) and standard errors are shown in the figure.

Table 4 Planetary and Stellar Parameters of Discovered Brown Dwarf Companions ($13 M_J < M_p \sin i < 80 M_J$) to Intermediate-mass Giants

Planet	$M_p \sin i$ (M_J)	a (AU)	P (day)	e	M_* (M_\odot)	$M_p \sin i / M_*$ (M_J / M_\odot)	[Fe/H]	Reference
HD 13189 b	14	1.5-2.2	472	0.27	2-6	2.3-7		Hatzes et al. (2005)
NGC 4349 No. 127 b	19.8	2.38	678	0.19	3.9	5.1	-0.12	Lovis & Mayor (2007)
11 Com b	19.4	1.29	326	0.23	2.7	7.2	-0.35	Liu et al. (2008)
BD +20 2457 b	21.42	1.45	380	0.15	2.8	7.7	-1.00	Niedzielski et al. (2009)
BD +20 2457 c *	12.47	2.01	622	0.18	2.8	4.5	-1.00	Niedzielski et al. (2009)
HD 119445 b	37.6	1.71	410	0.08	3.9	9.6	+0.04	Omiya et al. (2009)
HD 180314 b	22	1.4	396	0.26	2.6	8.5	+0.20	Sato et al. (2010)
HD 175679 b	37.3	3.4	1367	0.38	2.7	13.8	-0.14	This paper

* BD +20 2457 c has a minimum mass $M_p \sin i = 12.47 M_J$, very closed to the lower mass limit ($\sim 13 M_J$) of brown dwarf. Here we listed BD +20 2457 c as a brown dwarf companion.

2007; Johnson et al. 2010), HD 175679 b has the largest companion-to-host mass ratio ($M_p \sin i / M_* = 13.8 M_J / M_\odot$) among those discovered brown dwarfs around intermediate-mass giants, and hence fall in the region (a) in Figure 5 of Omiya et al. (2009), which is proposed to be a paucity of brown dwarf-mass companion around stars with $M_* = 1.5 - 2.7 M_\odot$.

Furthermore, HD 175679 b is the first brown dwarf candidate with semimajor axis $a > 2.5$ AU, and eccentricity $e > 0.3$ around evolved stars, displaying the diversity of substellar companions falling in the ‘brown dwarf desert’ regime. Brown dwarfs are thought to form by gravitational collapse (Bonnell &

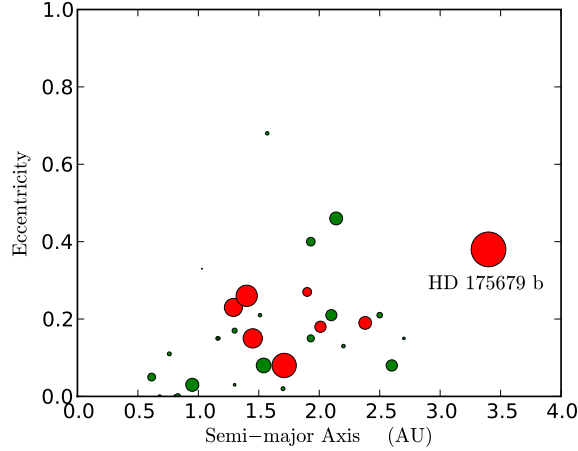


Fig. 3 Semi-major axes versus eccentricity of substellar companions around evolved intermediate-mass stars ($1.5 M_{\odot} \leq M \leq 5 M_{\odot}$). Green circles represent planetary companions, and red circles represent brown dwarf-mass companions, as listed in Table 4. Radius of circles are proportional to their companion-to-host mass ratios ($M_p \sin i / M_*$).

Bastien 1992; Bate 2000), or gravitational instability in protostellar disks (Boss 2000; Rice et al. 2003). The former scenario favors a wide variety of orbital eccentricity and small differences in mass between the host stars and their companions, which is contrary to the previous discoveries (e.g. Omiya et al. 2009; Sato et al. 2010). For the gravitational instability scenario, analytical models (e.g. Rafikov 2005, Matzner & Levin 2005) and numerical simulations (e.g. Stamatellos & Whitworth 2008) suggest that giant planets are formed at far more distant places ($\gtrsim 10$ AU), and a high eccentricity can be excited (e.g. Muto et al. 2011) in this scenario. On the other hand, super-massive companions with $M_p > 10 M_J$ can also form by core-accretion scenario in protoplanetary disks (Ida & Lin 2004; Alibert et al. 2005). But the wide metallicity span ($[\text{Fe}/\text{H}] = -1.0 \sim +0.2$) of host stars of discovered brown-mass companions implies they are inconsistent with the prediction of the core-accretion scenario that the probability of harboring planet is sensitive to the metallicity of a central star. Besides, the giant planets orbiting metal-poor stars discovered by Santos et al. (2010) and Moutou et al. (2011) suggest that long period giant planets are not rare around low-metallicity stars. It is difficult to say which scenario dominates the formation of brown dwarf mass companions due to the small number of discovered objects. However, the relatively large semimajor axis and relatively high eccentricity of HD 175679 b make it an important supplement to the parametric distribution of known brown dwarf companions. It also need to be emphasized that HD 175679 b has the longest orbital period (1367 days) among those ever discovered brown dwarf-mass companions to intermediate-mass giants. Does the long period companion tend to have higher eccentricity? Ongoing projects and future discoveries will lead to better understanding and characterizing properties of substellar companions falling in the brown dwarf desert.

Acknowledgements This research is based on data collected at Xinglong Station, which is operated by the National Astronomical Observatories, Chinese Academy of Sciences, and Okayama Astrophysical Observatory, which is operated by the National Astronomical Observatory of Japan (NAOJ). We thank Dr. Xiaojun Jiang, Hongbin Li, Feng Xiao, and Junjun Jia for their expertise and support in the Xinglong observations. We are grateful to all staff members of OAO for their support during the observations. This work was funded by the National Natural Science Foundation of China under grants 10821061 and 10803010 and Japan Society for the Promotion of Science under grant 08032011-000184 in the

framework of Joint Research Project between China and Japan. This research has made use of the SIMBAD database, operated at CDS, Strasbourg, France.

References

- Alibert Y., Mordasini C., Benz W., Winisdoerffer C., 2005, *A&A*, 434, 343
 Alonso A., Arribas S., Martínez-Roger C., 1999, *A&AS*, 140, 261
 Bate M. R., 2000, *MNRAS*, 314, 33
 Bonnell I., Bastien P., 1992, *ApJ*, 401, 654
 Boss A. P., 1997, *Science*, 276, 1836
 Boss A. P., 2000, *ApJ*, 536, L101
 Burkert A., & Ida S., 2007, *ApJ*, 660, 845
 Cumming A. et al., *PASP*, 120, 531
 Döllinger M. P. et al., 2009, *A&A*, 505, 1311
 ESA, 1997, *The Hipparcos and Tycho Catalogues*, 1239
 Fischer D. A., Valenti J., 2005, *ApJ*, 622, 1102
 Frink S., Mitchell D. S., Quirrenbach A., Fischer D. A., Marcy G. W., Butler R. P., 2002, *ApJ*, 576, 478
 Grether D., Lineweaver C., 2006, *ApJ*, 640, 1051
 Han Inwoo, Lee B. C., Kim K. M., Mkrtichian D. E., Hatzes A. P., & Valyavin G., 2010, *A&A*, 509, 24
 Hatzes A. P., Guenther E. W., Endl M., Cochran W. D., Döllinger M. P., & Bedalov A., 2005, *A&A*, 437, 743
 Ida S., & Lin D. N. C., 2004, *ApJ*, 604, 388
 Ida S., & Lin D. N. C., 2005, *ApJ*, 626, 1045
 Izumiura, H. 999, in *Proc. 4th East Asian Meeting on Astronomy*, ed. P. S. Chen (Kunming: Yunnan Observatory), 77
 Johnson J. A. et al. 2007, *ApJ*, 665, 785
 Johnson J. A. et al. 2008, *ApJ*, 675, 784
 Johnson J. A., Aller K. M., Howard A. W., & Crepp J. R., 2010, *PASP*, 122, 905
 Kambe E. et al., 2002, *PASJ*, 54, 865
 Kjeldsen H. & Bedding T. R., 1995, *A&A*, 293, 87
 Liu Y.-J. et al., 2008, *ApJ*, 672, 553
 Liu Y.-J., Sato B., Zhao G., & Ando H., 2009, *Research in Astronomy and Astrophysics*, 9, 1
 Liu, Y., Sato, B., Takeda, Y., Ando, H., & Zhao, G., 2010, *PASJ*, 62, 1071
 Lovis C., & Mayor M., 2007, *A&A*, 472, 657
 Marcy G. W., & Butler, R. P., 2000, *PASP*, 112, 137
 Matzner C. D. & Levin Y., 2005, *ApJ*, 628, 817
 Moutou C., et al., 2011, *A&A*, 527, A63
 Muto T., et al., 2011, *arxiv* 1106.0417
 Niedzielski A. et al., 2007, *ApJ*, 669, 1354
 Niedzielski A. et al., 2008, *ApJ*, 693, 276
 Niedzielski A., Nowak G., Adamow M., & Wolszczan A., 2009, *ApJ*, 707, 768
 Pasquini L. et al. 2007, *A&A*, 473, 979
 Omiya M. et al. 2009, *PASJ*, 61, 825
 Rafikov R. R., 2005, *ApJ*, 621, L69
 Rice W. K. M., et al., 2003, *MNRAS*, 346, L36
 Santos M. C. et al., 2010, *A&A*, 512, A47
 Sato B., Kambe E., Takeda Y., Izumiura H., & Ando H., 2002, *PASJ*, 54, 873
 Sato B. et al. 2003, *ApJ*, 597, L157
 Sato B. et al. 2005, *PASJ*, 57, 97
 Sato B. et al., 2007, *ApJ*, 661, 527

- Sato B. et al. 2008a, PASJ, 60, 539
Sato B. et al. 2008b, PASJ, 60, 1317
Sato B. et al. 2010, PASJ, 62, 1063
Setiawan J. et al. 2003, A&A, 398, L19
Setiawan J. et al. 2005, A&A, 437, L31
Stamatellos D. & Whitworth A. P., 2008, A&A, 480, 879
Takeda, Y., Sato, B., & Murata, D., 2008, PASJ, 60, 781
Yi, S. K., Kim, Y.-C., & Demarque, P., 2003, ApJS, 144, 259
Zhao G., & Li H.-B., 2001, ChJAA (Chin. J. Astron. Astrophys.), 1, 555